LETTERS IN BIOMATHEMATICS
An International Journal

Intercollegiate Biomathematics Alliance

RESEARCH ARTICLE

OPEN ACCESS

Analysis of Infected Population Threshold Exceedance in an SIR Epidemiological Model

Andrés David Báez-Sánchez, Nara Bobko

Department of Mathematics, Federal University of Technology, Av. Sete de Setembro, 3165, 80230-901, Curitiba, Paraná, Brazil.

ABSTRACT

Since the beginning of the COVID-19 outbreak, much attention has been given to the idea of *flattening the curve* of cases to reduce the harmful effects of an overloaded medical system. In this context, it is relevant to determine conditions to ensure that the health care threshold capacity will not be exceeded. If such a situation is unavoidable, it would be useful to effectively quantify the potential negative impact produced. In this paper, we consider an epidemiological SIR model and a positive threshold M. Using a parametric expression for the solution curve of the SIR model and the properties of the Lambert W function, we establish necessary and sufficient conditions on the basic reproduction number $\mathcal{R}_0$ to ensure that the infected population I does not exceed M. We also introduce and numerically analyze, five different quantities to measure the impact caused by a possible threshold exceedance.

ARTICLE HISTORY

Received October 6, 2020
Accepted June 1, 2021

KEYWORDS

SIR Epidemiological Model, Lambert W Function, Infected Population Threshold

1 Introduction

During the current COVID-19 outbreak, much attention has been given to the idea of *flattening the curve* of infection (Figure 1) to reduce the harmful effects of an overloaded medical system (Ferguson et al., 2020; Feng et al., 2020; Daud, 2021; Cooper et al., 2020).

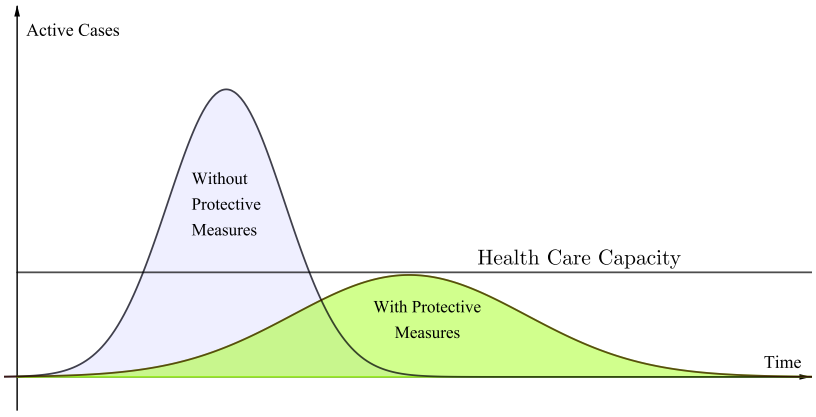

Figure 1: Flattening the curve.

As the number of active cases requiring hospitalization exceeds healthcare capacity, the disease's mortality rates rise, and there is a general decrease in the quality of medical care (Bigiani et al., 2020; Karaca-Mandic et al., 2020; Rossman et al., 2021).

It is desirable, therefore, to determine which specific conditions will ensure that the health care capacity will not be exceeded; and, if such a situation is unavoidable, it would be useful to have a way to quantify the negative impact produced.

CONTACT Andrés David Báez-Sánchez adsanchez@utfpr.edu.br

If one considers that a negative impact is produced any time the number of active cases reaches a certain threshold and that the more this number exceeds the threshold, the more damage is done to the health system as a whole, then, a possible way to quantify this damage could be obtained by *aggregating* the number of active cases above the threshold, whenever they occur. As an example, consider the area under the curve of active infected cases and above the threshold of health care capacity (the hatched area in Figure 2).

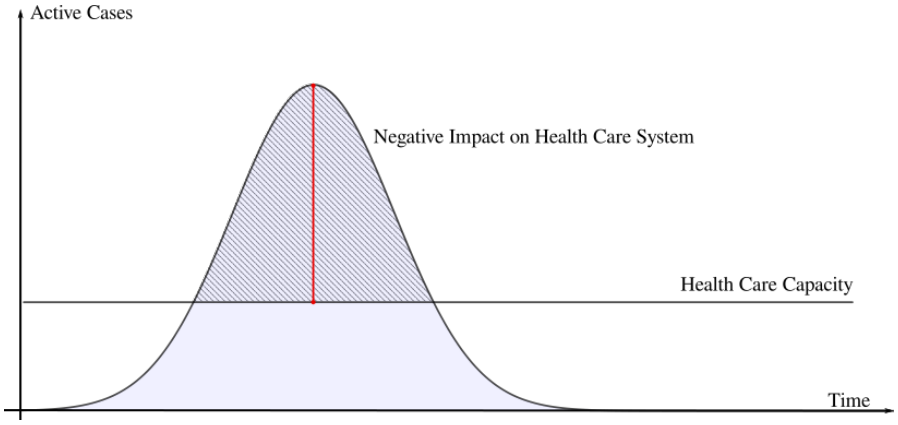

Figure 2: Measuring the negative impact on the Health Care System.

If one is only concerned about the peak of infection, another simple measurement of a negative impact can be obtained by the difference between the maximum number of active cases and the threshold of health care capacity (red line in Figure 2).

In general, note that, if one establishes some ideal parameter value that ensures that the peak of infections will be less than, or equal to, the health care capacity, one could use the difference between the current and the ideal value as a measurement for a negative impact. This difference, in some sense, answers the question: *How far from the ideal situation are we?*

In this paper, we consider an epidemiological SIR model and a positive threshold M. We establish necessary and sufficient conditions on the reproduction number $\mathcal{R}_0$ to ensure that the infected population does not exceed M. We also propose five different measures to quantify the impact caused by a possible threshold exceedance, based on the ideas of the aggregation of the exceeding infected cases and the difference between current and ideal parameter values.

Throughout this paper, we will use an exact parametric solution for the SIR model, based on the work of Harko et al. (2014), and we will also use the Lambert W function, also known as the product logarithm function (Corless et al., 1996).

Previous studies have considered the Lambert W function in the context of epidemiological models. In Reluga (2004); Wang (2010); Pakes (2015), the Lambert W function is used to express the final sizes of the epidemiological variables, and in Xiao et al. (2013); Wang et al. (2020), the Lambert W function is used to study an epidemiological model with a piecewise incidence rate. The usefulness of the Lambert W function in these studies, as well as in ours, lies in the fact that it can be used to express the solutions of some nonlinear equations in closed form, that cannot be solved otherwise in terms of elementary functions. We include some results and properties related to the Lambert W function in Appendix A and additional details and applications can be found in Corless et al. (1996); Lehtonen (2016).

The rest of this paper is organized as follows: Section 2 briefly recalls the epidemiological SIR model and presents a parametric solution following the results in Harko et al. (2014). In Section 3, we establish conditions for the basic reproduction number to ensure that the maximum of the infected population does not exceed the threshold M. In Section 4, we propose and analyze five different measures to quantify the impact caused by a possible threshold exceedance. Final considerations are presented in Section 5.

2 An epidemiological SIR model and its parametric solution

The main idea behind SIR models is to consider that a population N is divided into three disjoint categories or compartments: susceptible individuals, infected individuals, and removed individuals (recovered or deceased individuals), denoted by S, I, and R respectively, so $N = S + I + R$.

We consider the following SIR model,

$$\begin{aligned} \frac{dS}{dt} &= -\beta S I \\ \frac{dI}{dt} &= \beta S I - \gamma I \\ \frac{dR}{dt} &= \gamma I. \end{aligned} \tag{1}$$

The positive real numbers β and γ are interpreted as the infection rate and recovery rate, respectively. Note that, by adding equations in (1), we can obtain

$$\frac{dN}{dt} = \frac{dS}{dt} + \frac{dI}{dt} + \frac{dR}{dt} = 0.$$

Thus, we can consider $N(t) = S(t) + I(t) + R(t)$ constant for all t. Taking the standard definition of the basic reproduction number in the classical SIR model, given by $\mathcal{R}_0 = \frac{\beta N}{\gamma}$, we can rewrite (1) as

$$\begin{aligned} \frac{dS}{dt} &= -\frac{\gamma \mathcal{R}_0 S I}{N} \\ \frac{dI}{dt} &= \frac{\gamma \mathcal{R}_0 S I}{N} - \gamma I \\ \frac{dR}{dt} &= \gamma I. \end{aligned} \tag{2}$$

The basic reproduction number $\mathcal{R}_0$ has a fundamental role in the description of the equilibria stability in the classical SIR model. Within the limitations of the model, $\mathcal{R}_0$ can be interpreted as the number of new cases that one case generates, on average, within a completely susceptible population (Heffernan et al., 2005; Martcheva, 2015). Additional considerations regarding the interpretation of $\mathcal{R}_0$ can be found in Delamater et al. (2019); Li et al. (2011).

There is not an exact analytical solution of the SIR model (2) in terms of the parameter t. However, it is possible to obtain a parametric solution in terms of a new parameter u. Following the results obtained in Harko et al. (2014), a parametric solution for the model (2) can be written as

$$\begin{aligned} S(u) &= x_0 u \\ I(u) &= \frac{N}{\mathcal{R}_0} \ln u - x_0 u + N \\ R(u) &= -\frac{N}{\mathcal{R}_0} \ln u, \end{aligned} \tag{3}$$

where $u = e^{-\frac{\mathcal{R}_0}{N} R}$, and $x_0 = S(0) e^{\frac{\mathcal{R}_0}{N} R(0)}$.

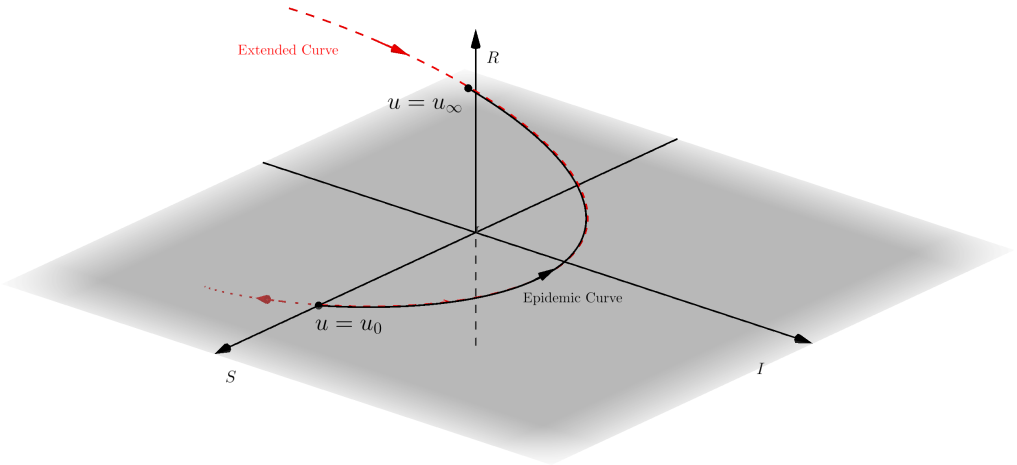

Figure 3: Parameter equations (3) describe a curve (red) that contains the solution curve of the epidemiological SIR model (black), but traversed in the opposite direction.

The parametric equations in (3) describe a curve in $\mathbb{R}^3$, which, for some specific values of u, corresponds precisely to the solution curve of (2) (for details see Harko et al., 2014). In particular, to properly describe the evolution of the removed population R, the parameter u should vary in such a way that R goes from $R(0)$ to $R_\infty := \lim_{t\to\infty} R(t)$. Thus, the third equation in (3) implies that in that case, u varies from $u_0 = e^{-\frac{\mathcal{R}_0}{N}R(0)}$ to $u_\infty = e^{-\frac{\mathcal{R}_0}{N}R_\infty}$.

Note that u was defined as a decreasing function of R and also that R is an increasing function of t. Therefore, the parameter u must decrease to properly describe the solution curve of (2) in the *time-forward direction*. In fact, as $0 \le R(0) \le R_\infty \le N$, we have that $e^{-\mathcal{R}_0} \le u_\infty \le u_0 \le 1$. If the parameter u varies from 0 to ∞, Equations (3) describe a curve in $\mathbb{R}^3$ that contains the solution of the model (1), but the curve is traversed in the opposite direction (Figure 3).

3 Controlling the maximum of the infected population

Let M be a positive constant such that $M < N$. We will consider M as a threshold that, ideally, must not be exceeded by the active infected population. In this section, we aim to obtain conditions to ensure that $I_{\max} \le M$, where $I_{\max}$ denotes the maximum value of the infected population I.

From now on, we consider that $S(0) > 0$ and $I(0) > 0$; so, $I(t) \neq 0$ for all $t > 0$. The following lemma establishes a sufficient condition for the basic reproduction number $\mathcal{R}_0$ to ensure that $I_{\max} \le M$.

Lemma 1. *If* $\mathcal{R}_0 \le \frac{N}{S(0)}$ *and* $I(0) \le M$, *or if* $\frac{N}{S(0)} < \mathcal{R}_0 \le \frac{N}{N-M}$, *then* $I_{\max} \le M$.

Proof. Note first that, because we are considering $I \neq 0$, the second equation in (2) implies that, $\frac{dI}{dt} = 0$ if, and only if, $S = \frac{N}{\mathcal{R}_0}$; I is increasing if, and only if, $S > \frac{N}{\mathcal{R}_0}$; and I is decreasing if, and only if, $S < \frac{N}{\mathcal{R}_0}$. Note also, from the first and third equations in (2), that S and R are non-increasing and non-decreasing functions of t, respectively.

Hence, if $\mathcal{R}_0 \le \frac{N}{S(0)}$ and $I(0) \le M$, then $S(0) \le \frac{N}{\mathcal{R}_0}$ and I is not increasing for all $t \ge 0$. Therefore, $I_{\max}$ is already attained at $I(0)$; so, $I_{\max} = I(0) \le M$.

On the other hand, if $\frac{N}{S(0)} < \mathcal{R}_0$, then I is increasing until it reaches its maximum value $I_{\max} = I(t^*)$, for some t^* satisfying $\frac{dI}{dt}(t^*) = 0$, which implies,

$$S(t^*) = \frac{N}{\mathcal{R}_0}. \tag{4}$$

From the fact that $R(t^*) \ge 0$, and $N = S(t) + I(t) + R(t)$, it follows that

$$I_{\max} = I(t^*) \le R(t^*) + I(t^*) = N - S(t^*) = N - \frac{N}{\mathcal{R}_0} = N\left(1 - \frac{1}{\mathcal{R}_0}\right). \tag{5}$$

Finally, note that if $\mathcal{R}_0 \le \frac{N}{N-M}$, then $N\left(1 - \frac{1}{\mathcal{R}_0}\right) \le M$ and, thus, from (5), we can conclude that if $\mathcal{R}_0 \le \frac{N}{N-M}$, then $I_{\max} \le M$. □

Lemma 1 provides an easily verifiable condition on $\mathcal{R}_0$ to ensure that the threshold M will not be exceeded. However, since it is only a sufficient condition based on upper bounds on $I_{\max}$, it can be a very restrictive condition on $\mathcal{R}_0$. Furthermore, it does not provide information on the value of $I_{\max}$ if the condition is not satisfied. In the following result, we use the parametric solution (3) to obtain an expression for $I_{\max}$ that will allow us to establish a more robust condition on $\mathcal{R}_0$ to control $I_{\max}$.

Proposition 1. $I_{\max} \le \frac{N}{\mathcal{R}_0}\left(\ln\left(\frac{N}{\mathcal{R}_0 S(0)}\right) - 1\right) - R(0) + N$ *and, if* $\mathcal{R}_0 \ge \frac{N}{S(0)}$, *the equality holds.*

Proof. Let us consider the parametric equations (3). Recall that, when u varies on the interval $(0, \infty)$, equations (3) describe an extended curve which contains the solution curve of (1), but is traversed in the opposite direction. This part of the curve corresponds to u varying on the interval $[u_\infty, u_0] \subset (0, \infty)$. Note, however, that the maximum value of I on this curve does not depend on the specific parametrization, nor on the curve orientation.

From the second equation in (3), we have that

$$\frac{dI}{du} = \frac{N}{\mathcal{R}_0 u} - x_0 \quad \text{and} \quad \frac{d^2I}{du^2} = -\frac{N}{\mathcal{R}_0 u^2} < 0. \tag{6}$$

Thus, I is a strictly concave function on u with a unique global maximum attained in $u^* = \frac{N}{\mathcal{R}_0 x_0}$. Furthermore, if $u < \frac{N}{\mathcal{R}_0 x_0}$, then I is strictly increasing, and if $u > \frac{N}{\mathcal{R}_0 x_0}$, I is strictly decreasing.

The maximum possible value for I along the extended curve, therefore, is given by

$$\begin{aligned} I(u^*) &= \frac{N}{\mathcal{R}_0}\ln\left(\frac{N}{\mathcal{R}_0 x_0}\right) - \frac{x_0 N}{\mathcal{R}_0 x_0} + N \\ &= \frac{N}{\mathcal{R}_0}\left(\ln\left(\frac{N}{\mathcal{R}_0 x_0}\right) - 1\right) + N \\ &= \frac{N}{\mathcal{R}_0}\left(\ln\left(\frac{N}{\mathcal{R}_0 S(0)}\right) - 1\right) - R(0) + N, \end{aligned}$$

where the last equality is obtained by using that $x_0 = S(0)e^{\frac{\mathcal{R}_0}{N}R(0)}$. Note that $I(u^*)$ is not necessarily equal to the maximum number of infected $I_{\max}$, but we must, indeed, have that, $I_{\max} \leq I(u^*)$. The equality will hold if, and only if, the global maximum of I is attained in the part of the curve corresponding to the epidemic, i.e. if, and only if, $u^* \in [u_\infty, u_0]$. If $\mathcal{R}_0 \geq \frac{N}{S(0)}$, then $\frac{N}{\mathcal{R}_0 S(0)} \leq 1$; thus,

$$u^* = \frac{N}{\mathcal{R}_0 x_0} = \frac{N}{\mathcal{R}_0 S(0)} e^{-\frac{\mathcal{R}_0}{N}R(0)} \leq e^{-\frac{\mathcal{R}_0}{N}R(0)} = u_0.$$

If $u_* < u_\infty \leq u_0$, then u_∞ and u_0 would also be on the decreasing side of I; so $I(u_\infty) \geq I(u_0)$. The last inequality would be absurd, since $I(u_0) = I(0) > 0$ and $I(u_\infty) = \lim_{t\to\infty} I(t)$ which, in the case of the SIR model (1), is equal to zero. Hence, we conclude that if $\mathcal{R}_0 \geq \frac{N}{S(0)}$, then $u^* \in [u_\infty, u_0]$ and, therefore, in this case, $I_{\max}$ and $I(u_*)$ must coincide, i.e.,

$$I_{\max} = \frac{N}{\mathcal{R}_0}\left(\ln\left(\frac{N}{\mathcal{R}_0 x_0}\right) - 1\right) + N = \frac{N}{\mathcal{R}_0}\left(\ln\left(\frac{N}{\mathcal{R}_0 S(0)}\right) - 1\right) - R(0) + N. \tag{7}$$

□

Equality (7) can also be obtained without using the parametric equations (3), by solving a separable ODE obtained by dividing the first equation in (1) by the second one (see, for example, Weiss, 2013, Section 2.2.7).

Equality (7) can be used to easily check if $I_{\max}$ will or will not exceed M, for some given values of the reproduction number, initial conditions, and M. Furthermore, Equality (7) can be used to estimate conditions on the parameters or on the initial conditions, implying that $I_{\max} \leq M$. In particular, the next proposition uses Equality (7) and the Lambert W function to determine a necessary and sufficient condition on $\mathcal{R}_0$ to ensure that $I_{\max} \leq M$.

Proposition 2. *Consider that $\mathcal{R}_0 \geq \frac{N}{S(0)}$ and $I(0) < M < S(0) + I(0)$. Then $I_{max} \leq M$ if, and only if,*

$$\mathcal{R}_0 \leq N\frac{W_{-1}\left(\frac{M-N+R(0)}{S(0)e}\right)}{M - N + R(0)}, \tag{8}$$

where W_{-1} denotes the lower branch of the Lambert W function.

Proof. The condition $\mathcal{R}_0 \geq \frac{N}{S(0)}$ allows us to consider the Equality (7). The inequality $I(0) < M < S(0) + I(0)$ means that M has not been attained at initial conditions, and also that M is not impossible to be attained, because $S(0) + I(0)$ is the maximum number of the population that has not yet been removed and may eventually become infected at some point.

From the second equality in (7), note that

$$\frac{dI_{\max}}{d\mathcal{R}_0} = -\frac{N}{\mathcal{R}_0^2}\left(\ln\left(\frac{N}{\mathcal{R}_0 S(0)}\right) - 1\right) - \frac{N}{\mathcal{R}_0}\left(\frac{\mathcal{R}_0 S(0)}{N}\frac{N}{\mathcal{R}_0^2 S(0)}\right) = \frac{N}{\mathcal{R}_0^2}\ln\left(\frac{\mathcal{R}_0 S(0)}{N}\right). \tag{9}$$

So, $I_{\max}$ is an increasing function on $\mathcal{R}_0$ when $\mathcal{R}_0 > \frac{N}{S(0)}$. Additionally, note from (7) that, if $\mathcal{R}_0 \to \infty$, then we have that $I_{\max} \to N - R(0) = S(0) + I(0)$. So, the condition $I(0) < M < S(0) + I(0)$ implies that M is, in fact, an attainable value for $I_{\max}$, i.e. there exists a value $\mathcal{R}_0^* > \frac{N}{S(0)}$ such that $I_{\max} = I_{\max}(\mathcal{R}_0^*) = M$. Using the Lambert W function (See Appendix A for details), it is possible to determine this value. From Equation (7), we have that

$$\begin{aligned} I_{\max} = M \quad &\Rightarrow \quad \frac{N}{\mathcal{R}_0^*}\left(\ln\left(\frac{N}{\mathcal{R}_0^* S(0)}\right) - 1\right) = M + R(0) - N \\ &\Rightarrow \quad \frac{N}{\mathcal{R}_0^* S(0)}\ln\left(\frac{N}{\mathcal{R}_0^* S(0)}\right) = \frac{N}{\mathcal{R}_0^* S(0)} + \frac{M + R(0) - N}{S(0)} \\ &\Rightarrow \quad v\ln v = v + b, \end{aligned}$$

with $v = \frac{N}{\mathcal{R}_0^* S(0)}$ and $b = \frac{M+R(0)-N}{S(0)}$. According to Lemma 4 in A, the solutions to the equation $v \ln v = v + b$ have the form

$$v = \frac{b}{W(be^{-1})}.$$

Since $be^{-1+1} = b = \frac{M+R(0)-N}{S(0)}$, the condition $I(0) < M < S(0) + I(0)$ implies that $-1 < b < 0$. Hence, Lemma 4 also implies that $v \ln v = v + b$ has two solutions, each one corresponding to a specific branch of the function W. One of these solutions is precisely given by $v = \frac{N}{\mathcal{R}_0^* S(0)} \leq 1$; so, we must have for a certain branch of W that

$$\frac{b}{W(be^{-1})} \leq 1 \tag{10}$$

for b in $(-1, 0)$. This is only possible for the lower branch of the Lambert W function and, thus, we conclude that $\frac{b}{W_{-1}(be^{-1})} = \frac{N}{\mathcal{R}_0^* S(0)}$. Therefore,

$$\mathcal{R}_0^* = N \frac{W_{-1}\left(\frac{M-N+R(0)}{S(0)e}\right)}{M - N + R(0)}. \tag{11}$$

Finally, as we have established that $I_{\max}$ is an increasing function on $\mathcal{R}_0$ and we have that $I_{\max}$ attains M at $\mathcal{R}_0^*$, then the condition $I_{\max} \leq M$ will be satisfied if, and only if, $\mathcal{R}_0 \leq \mathcal{R}_0^*$, and the desired result follows from Equation (11). □

Example 1. To illustrate the result obtained in Proposition 2, consider a scenario with the total population $N = 100$, the recovery rate $\gamma = 1/3$, the initial conditions $S(0) = 99$, $I(0) = 1$, $R(0) = 0$, and a threshold M equal to 10, corresponding to 10% of the total population. In this case, using equation (11), we obtain a critical value $\mathcal{R}_0^* \approx 1.7$. The corresponding curve of infected cases is pictured in orange in Figure 4. Note that, as expected, the maximum value of active infected cases, I_{max}, corresponds exactly to M.

In Figure 4, the curves of infected cases corresponding to a basic reproduction number 10% higher (purple line), and 10% lower (green) than the critical value $\mathcal{R}_0^*$ are also pictured. As expected, the values of $I_{\max}$ are higher and lower than M, respectively.

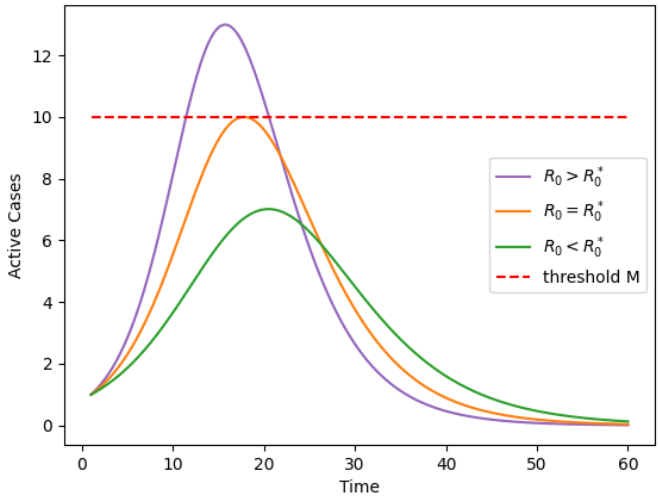

Figure 4: Curves of infected individuals for different values of $\mathcal{R}_0$, illustrating different scenarios concerning the threshold M (red dashed line). As in Example 1, the total population considered is $N = 100$ and M is 10% of N ($M = 10$), resulting in the critical reproduction number $\mathcal{R}_0^* \approx 1.7$.

An additional consequence of Propositions 1 and 2 is that, when there is an estimation of the value of I_{max}, one can use Equation (11) to obtain *a posteriori* estimation for $\mathcal{R}_0$. This is established explicitly in the following corollary and will be used in the numerical example in Subsection 4.2.2.

Corollary 1. *If* $I(0) > 0$ *and* $\frac{dI}{dt}(0) > 0$, *then* $\mathcal{R}_0$ *can be written in terms of* I_{max} *as*

$$\mathcal{R}_0 = N\frac{W_{-1}\left(\frac{I_{max}-N+R(0)}{S(0)e}\right)}{I_{max}-N+R(0)}. \tag{12}$$

Proof. If $I(0) > 0$ and $\frac{dI}{dt}(0) > 0$, then the second equation in (2) implies that $\mathcal{R}_0 \geq \frac{N}{S(0)}$ and the result follow from Equation (11), considering $M = I_{\max}$. □

4 Quantifying the impact of threshold exceedance

In this section, we propose and compare different measures to quantify the impact produce by exceeding the threshold M. Using Propositions 1 and 2, we have a way to quantify how far from M the value $I_{\max}$ would be and how far $\mathcal{R}_0$ is from its maximum acceptable value. Those are precisely the motivations behind quantities Q_1 and Q_2, defined by:

$$Q_1 = \mathcal{R}_0 - \mathcal{R}_0^* = \mathcal{R}_0 - N\frac{W_{-1}\left(\frac{M-N+R(0)}{S(0)e}\right)}{M-N+R(0)}, \tag{13}$$

and

$$Q_2 = I_{max} - M = \frac{N}{\mathcal{R}_0}\left(\ln\left(\frac{N}{\mathcal{R}_0 S(0)}\right) - 1\right) - R(0) + N - M. \tag{14}$$

Figures 5(a) and 5(b) illustrate quantities Q_1 and Q_2. The blue line in Figure 5(a) corresponds to the value of I_{max} calculated for different values of $\mathcal{R}_0$. Note that, at $\mathcal{R}_0^*$, we have that $I_{max} = M$. The value of Q_1 for a specific $\mathcal{R}_0$ is the difference between $\mathcal{R}_0$ and $\mathcal{R}_0^*$. The blue line in Figure 5(b) corresponds to the values of $I(t)$ and the maximum peak of this curve, I_{max}, is highlighted by the black dashed line. The value of Q_2 is the difference between I_{max} and M.

The quantities Q_1 and Q_2 only consider the impact on the epidemic peak, without explicitly considering the total impact of exceeding the threshold. To take this into account, we can *aggregate* all threshold exceedances, using some form of integration. For example, we can integrate the difference $I - M$ precisely over the time interval where I is greater than M. This is the motivation behind quantity Q_3, defined as

$$Q_3 = \int_{t_i}^{t_f} (I(t) - M)\, dt, \tag{15}$$

where $t_i \leq t_f$ are values of t such that $I(t_i) = M = I(t_f)$ and $M < I_{\max}$, i.e. $[t_i, t_f]$ is the interval where I is greater than M. Quantity Q_3 is illustrated in Figure 5(c).

The quantity Q_3 is a natural expression for impact quantification, however, note that there is not an analytical expression for I in terms of t, neither are there closed forms for the limits of integration t_i and t_f. Therefore, Q_3 can only be estimated numerically.

A similar integration-based measure can be considered, related to the parametric equations in (3), with an analogous interpretation, but expressed in terms of the parameter u. This is the motivation behind the quantity Q_4, defined as follows:

$$Q_4 = \int_{u_f}^{u_i} (I(u) - M)\, du = \int_{u_f}^{u_i} \left(\frac{N}{\mathcal{R}_0}\ln u - x_0 u + N - M\right) du = \left(\frac{N}{\mathcal{R}_0}(u\ln u - u) - \frac{x_0 u^2}{2} + (N-M)u\right)\Bigg|_{u_f}^{u_i}, \tag{16}$$

where $u_f \leq u_i$ are such that $I(u_f) = M = I(u_i)$. These values u_f and u_i are the endpoints of the interval where $I(u)$ exceeds M, so, they are analogous, in the parameter u, to t_i and t_f. Unlike quantity Q_3, there exists a closed form for Q_4 and, as we will see in Subsection 4.1, there also exists closed form expressions for u_f and u_i in terms of the Lambert W function. Quantity Q_4 is illustrated in Figure 5(d). Note that, in Figure 5(d), I is varying according to the parameter u, while in Figure 5(c), I is varying according to t.

While Q_3 and Q_4 are defined in similar ways as definite integrals of a real function, their values are not necessarily equal, since they are based on different parametrizations of the epidemic curve. However, it is possible to define an integration-based measure that does not depend on parametrization, using the following line integral on the three-dimensional extended curve:

$$Q_5 = \int_C f \cdot ds,$$

where C corresponds to the part of the epidemic curve where I is greater or equal to M and f is the scalar field defined by $f = I - M$. The quantity Q_5 resembles Q_3 and Q_4 and can be considered a natural expression to quantify the global threshold

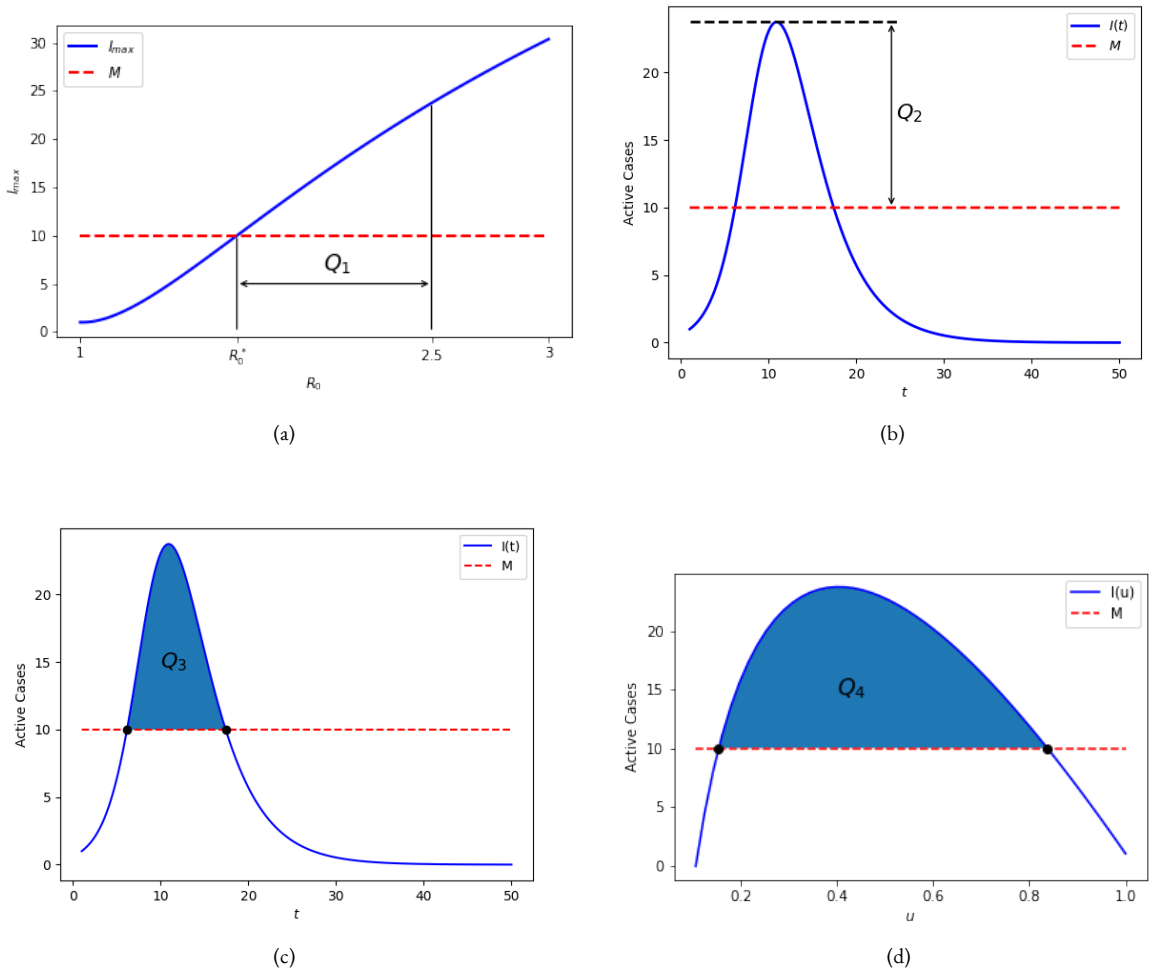

Figure 5: Representation of quantities Q_1, Q_2, Q_3, and Q_4, for the parameters $N = 100$, $\gamma = 1/3$, $\mathcal{R}_0 = 2.5$, $S(0) = N - 1$, $I(0) = 1$, $R(0) = 0$, and M equal to 10% of N ($M = 10$). The threshold M is represented by the red dashed line.

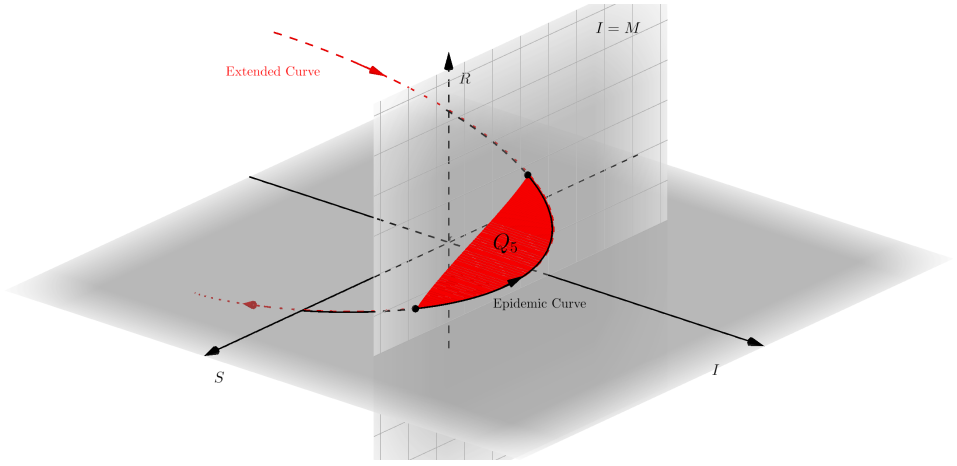

Figure 6: Line Integral Q_5 as a measure for threshold exceedance quantification.

exceedance, when considering the three-dimensional epidemic curve and the area of the surface determined by the curve and the plane $I = M$ (see Figure 6).

The quantity Q_5 does not depend on the parametrization or the orientation of C because it is defined as the line integral of a scalar field on a smooth curve. Hence, to calculate Q_5, we could use any parametrization. In particular, we have that

$$Q_5 = \int_C f \cdot ds = \int_{t_i}^{t_f} (I(t) - M)|r_t'(t)|\, dt = \int_{u_f}^{u_i} (I(u) - M)|r_u'(u)|\, du, \tag{17}$$

where t_i, t_f, u_f, and u_i are defined as before and r_t and r_u are parametrizations of the epidemiological curve in terms of t and u, respectively. As previously discussed, there are no closed expressions for $I(t)$, t_i, or t_f; nor are there any for r_t. However, note that, for the parameter u, the expressions for $r_u(u)$ and $I(u)$ are given precisely by Equations (3). Thus, Q_5 can be expressed as

$$Q_5 = \int_{u_f}^{u_i} (I(u) - M)|r_u'(u)|\, du = \int_{u_f}^{u_i} \left(\frac{N}{\mathcal{R}_0} \ln u - x_0 u + N - M\right) \sqrt{2\left(x_0^2 + \frac{N}{\mathcal{R}_0 u}\left(\frac{N}{\mathcal{R}_0 u} - x_0\right)\right)}\, du. \tag{18}$$

In subsection 4.2.1, we will use numerical examples to compare the quantities introduced above and to illustrate the influence of variations on parameters $\mathcal{R}_0$ and M. Before that, however, in the next subsection, we show that u_f and u_i can be expressed in closed form, in terms of the Lambert W function.

4.1 Estimation of u_i and u_f

The effective computation of quantities Q_4 in (16) and Q_5 in (18) requires the determination of the values of u_i and u_f, such that $I(u_f) = M = I(u_i)$. In terms of Equations (3), we seek solutions $u \in (0, \infty)$, for the equation

$$I(u) = \frac{N}{\mathcal{R}_0} \ln u - x_0 u + N = M. \tag{19}$$

We have already established that the maximum possible value for I is given by $\frac{N}{\mathcal{R}_0}\left(\ln\left(\frac{N}{\mathcal{R}_0 x_0}\right) - 1\right) + N$; so, Equations (19) cannot have solutions, if M is larger than this quantity. The following proposition, which uses Lemma 3 in Appendix A, can be used to reach the same conclusion; but, most importantly, it will allow us to obtain a closed form for the solutions of (19), and will allow us to express u_f and u_i, in terms of the Lambert W function.

Proposition 3. *Let M be a positive real number, where $M \leq N$ and consider $S(0) > 0$.*

- *If $M < \frac{N}{\mathcal{R}_0}\left(\ln\left(\frac{N}{\mathcal{R}_0 x_0}\right) - 1\right) + N$, then I attains the value M in two values of u, considering the two branches of W in the expression*

$$u = \frac{W\left(-x_0 \frac{\mathcal{R}_0}{N} e^{\frac{\mathcal{R}_0}{N}(M-N)}\right)}{-x_0 \frac{\mathcal{R}_0}{N}} = \frac{W\left(-\frac{\mathcal{R}_0}{N} S(0) e^{\frac{\mathcal{R}_0}{N}(R(0)+M-N)}\right)}{-\frac{\mathcal{R}_0}{N} S(0) e^{\frac{\mathcal{R}_0}{N} R(0)}}. \tag{20}$$

- *If $\frac{N}{\mathcal{R}_0}\left(\ln\left(\frac{N}{\mathcal{R}_0 x_0}\right) - 1\right) + N < M$, then I never reaches the value M.*

Proof. From Equation (19), we have that

$$\frac{N}{\mathcal{R}_0} \ln u - x_0 u + N = M \quad \Rightarrow \quad \ln u = \frac{\mathcal{R}_0}{N} x_0 u + \frac{\mathcal{R}_0}{N}(M - N);$$

so, the expression (20) for the solutions u, when they exist, can be obtained from Lemma 3, for $a = \frac{\mathcal{R}_0 x_0}{N}$ and $b = \frac{\mathcal{R}_0}{N}(M - N)$.

Let us analyze if, under the conditions considered, Equation (20) has two solutions. The condition for the existence of two solutions is given in Lemma 3 by $0 < ae^{b+1} < 1$, which, in this case, is equivalent to

$$0 < \frac{\mathcal{R}_0 x_0}{N} e^{\frac{\mathcal{R}_0}{N}(M-N)+1} < 1.$$

The left side inequality is immediately satisfied because $x_0 > 0$, when $S(0) > 0$. The right side is equivalent to

$$\begin{aligned} \frac{\mathcal{R}_0 x_0}{N} e^{\frac{\mathcal{R}_0}{N}(M-N)+1} < 1 \quad &\Rightarrow \quad e^{\frac{\mathcal{R}_0}{N}(M-N)+1} < \frac{N}{\mathcal{R}_0 x_0} \\ &\Rightarrow \quad \frac{\mathcal{R}_0}{N}(M-N) + 1 < \ln\left(\frac{N}{\mathcal{R}_0 x_0}\right) \\ &\Rightarrow \quad M < \frac{N}{\mathcal{R}_0}\left(\ln\left(\frac{N}{\mathcal{R}_0 x_0}\right) - 1\right) + N, \end{aligned}$$

which is precisely our hypothesis. By the same reasoning, the inequality $\frac{N}{\mathcal{R}_0}\left(\ln\left(\frac{N}{\mathcal{R}_0 x_0}\right)-1\right)+N<M$ is equivalent to $1<ae^{b+1}$, which, by Lemma 3, implies that Equation (19) has no solutions. □

4.2 Numerical examples

In this section, we illustrate some of the results obtained in two ways. First, we analyze different characteristics of the quantities Q_i, numerically, based on synthetic data. Then, we present an illustration of the estimation of quantity Q_4 and *a posteriori* estimation of $\mathcal{R}_0$, based on COVID-19 data from the city of Curitiba, Brazil.

The values of Q_1 and Q_2 were calculated using Equation (13) and (14), respectively. The value of Q_4 was calculated using the right side of (16), where the integration extremes, u_i and u_f, were obtained by Equation (20). The values of Q_3 and Q_5 were calculated using numerical approximations. For Q_3, we use Equation (15) and a numerical method of integration. The values of $I(t)$ were computed via a numerical solution of the differential equations in model (2) and the extremes of the integration interval were obtained by a numerical search among the discretized values of $I(t)$. For Q_5, we use the right side of Equation (18) and also a numerical integration method. The extremes of the integration interval, however, were calculated by Equation (20). Note that, in this case, there is no need for a numerical solution for the ODE system. All numerical calculations were performed in Python, using *lambertw* and *odeint* from the module *SciPy*, and *trapz* from *NumPy*.

4.2.1 Comparison between the quantities Q_i

Although the quantities presented in this paper all measure the impact of exceeding the threshold M, each one does it differently. To illustrate these differences, we present some numerical comparisons between the quantities. Note that, the basic reproduction number $\mathcal{R}_0$ and the threshold M, play fundamental roles in the dynamics and, consequently, in the values of quantities Q_i.

Figure 7 illustrates this by showing some heat maps of the intensity for each quantity Q_i and different values of $\mathcal{R}_0$ and M. At first glance, the quantities behave similarly with respect to variations in M and $\mathcal{R}_0$. As expected, we see low intensity for small $\mathcal{R}_0$ and large M, and a gradual increase in intensity as $\mathcal{R}_0$ increases or M decreases. Maximum intensity is attained for the highest values of $\mathcal{R}_0$ and the lowest values of M. Note, however, the difference in scale for each quantity.

A closer look at each quantity allows us to observe slightly different behaviors. Note, for example, that even for a low fixed M (such as $M = 3.75$), Q_3 has a very high intensity even at low $\mathcal{R}_0$ values, while Q_5 will only increase intensity significantly, for higher values of $\mathcal{R}_0$.

Figure 8 shows the quantities and their derivatives as functions of $\mathcal{R}_0$. Except for Q_1, which has a constant derivative, all other quantities have a derivative going to zero for large values of $\mathcal{R}_0$. This can be interpreted as a sensitivity loss for variations in $\mathcal{R}_0$, when $\mathcal{R}_0$ increases. This sensitivity loss evolves in different ways for each quantity.

All quantities have different value scales, hence, to compare them simultaneously over an interval, we can normalize their values with respect to the maximum value attained. To illustrate this kind of comparison, Figure 9(a) presents the normalized values for all quantities and Figure 9(b) shows the logarithmic derivatives of the quantities with respect to $\mathcal{R}_0$, that is, the quotient between $\frac{dQ_i}{d\mathcal{R}_0}$ and Q_i, for $i = 1, 2, 3, 4$ or 5. In this case, from Figure 9(a), we can establish that Q_3 approaches its maximum value comparatively faster than the other quantities, and, from Figure 9(b), that Q_5 is slightly more sensitive for small values of $\mathcal{R}_0$ than the other quantities.

4.2.2 Estimation of $\mathcal{R}_0$ and Q_4 in the city of Curitiba, Brazil

In this section we consider real data related to the pandemic of COVID-19 from Curitiba, the state capital of Paraná, Brazil.

It is worth noting that the estimates presented here are only intended to illustrate the potential use of some of the results presented in this article, and do not aim to provide a precise depiction of $\mathcal{R}_0$ for such a complex scenario as the COVID-19 pandemic. The results must also be considered within the limitations of the simple SIR model.

We consider the data made available by the Municipal Health Department of Curitiba (SMS, 2021), for the period from February to April 2021. This period corresponds to one of the COVID-19 *waves* in Curitiba. The I_{max} considered was the maximum number of active cases registered in this period ($I_{max} = 14271$). The total population was considered as $N = 1948626$, which corresponds to the estimate of Curitiba's population in 2020 (IBGE, 2021). The initial values of S, I, and R were: $S(0) = 1791069$, $I(0) = 5956$, and $R(0) = 151601$. This value of $I(0)$ corresponds to the number of active cases at the beginning of the period in question. The value of $R(0)$ was obtained by adding the cumulative number of registered cases and the number of vaccinated people at the beginning of the period, and then subtracting the value of $I(0)$. Finally, $S(0)$ was obtained by $N - I(0) - R(0)$.

Using this data and Equation (12), we obtain the *a posteriori* estimation for the corresponding basic reproduction number as $\mathcal{R}_0 = 1.2019$. Although this estimate of $\mathcal{R}_0$ requires prior knowledge of I_{max}, it can be relevant to study the variation of $\mathcal{R}_0$ in different locations, or even in the same place, but for different periods to compare different waves. This could help policy makers, to adjust preventive measures when facing new outbreaks of COVID-19 or other infectious diseases.

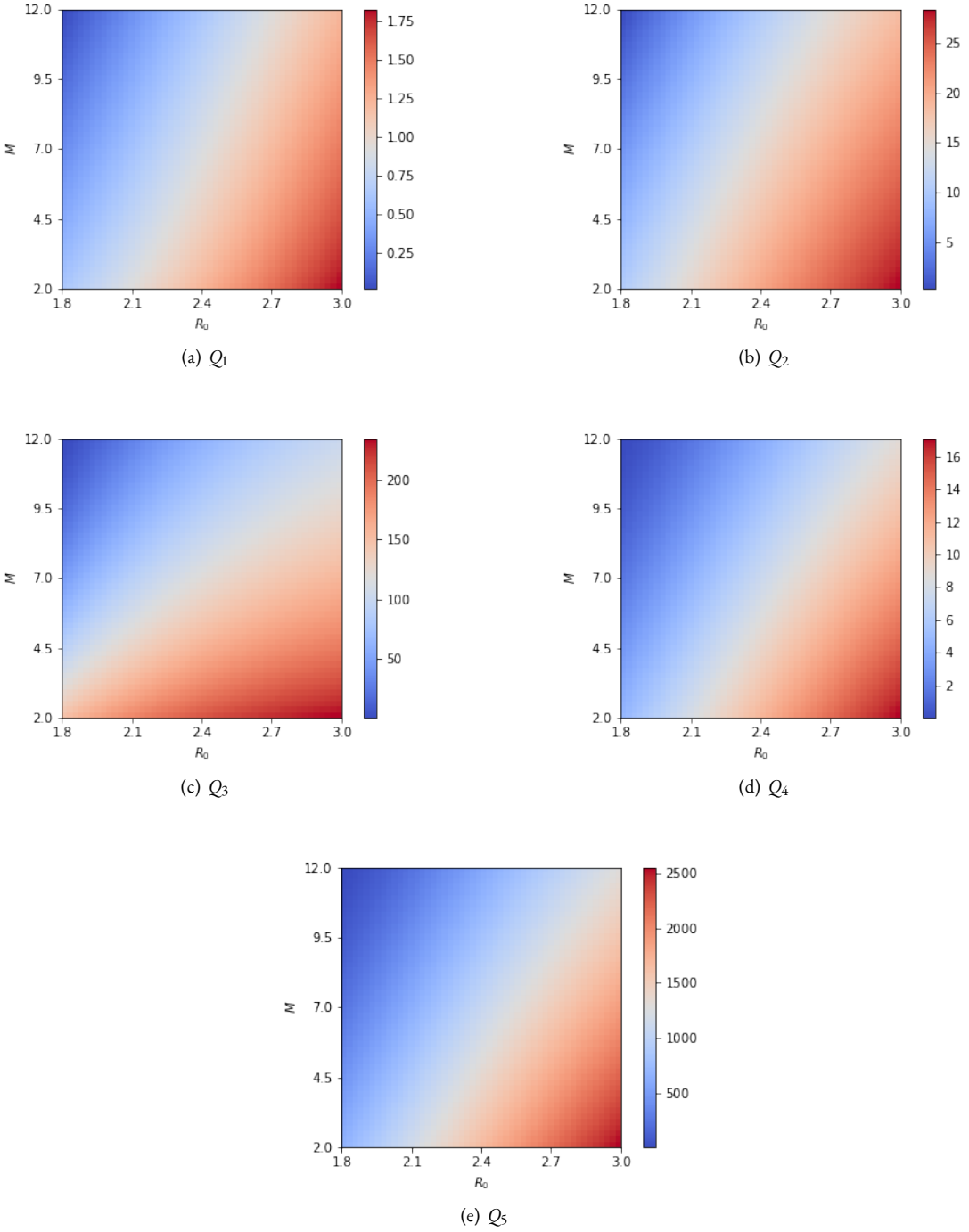

(a) Q_1 (b) Q_2

(c) Q_3 (d) Q_4

(e) Q_5

Figure 7: Heat maps for quantities $Q_i, i = 1, \ldots, 5$, for different values of $\mathcal{R}_0$ and M, with $N = 100, \gamma = 1/3, S(0) = N - 1$, $I(0) = 1, R(0) = 0, M \in [2, 12]$ and $\mathcal{R}_0 \in [1.8, 3]$.

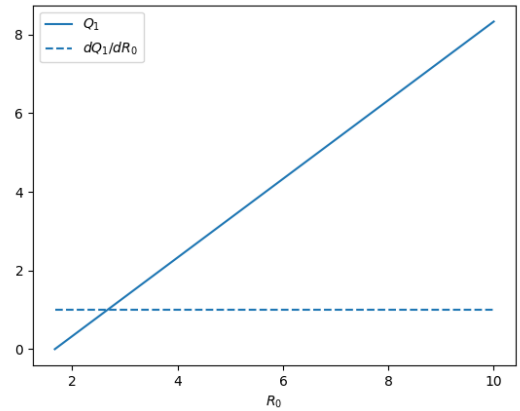

(a) Q_1

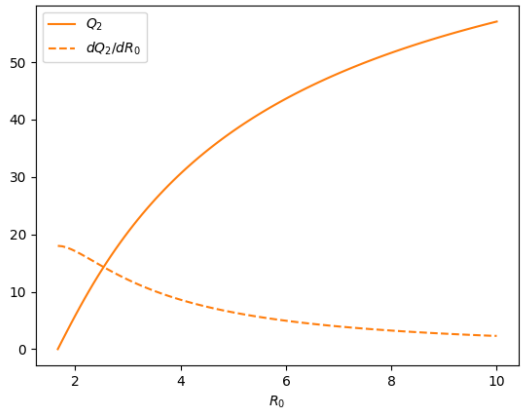

(b) Q_2

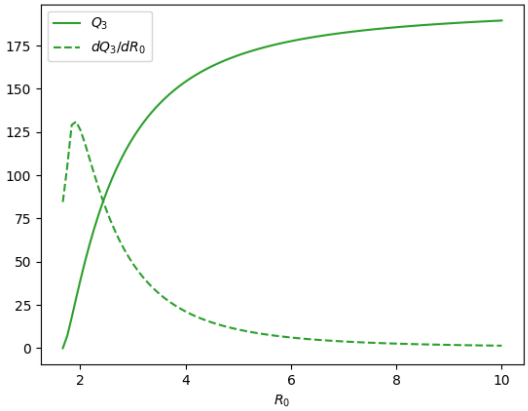

(c) Q_3

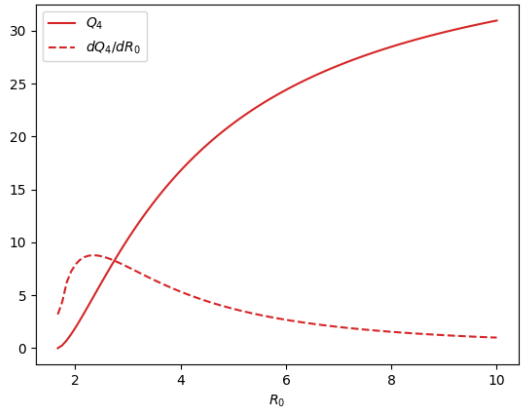

(d) Q_4

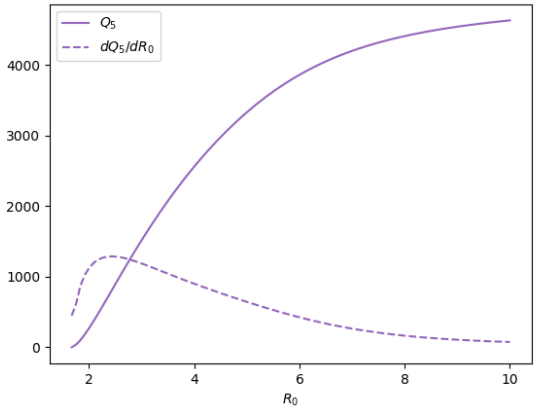

(e) Q_5

Figure 8: In solid lines, values of the quantities Q_1 (blue), Q_2 (orange), Q_3 (green), Q_4 (red), and Q_5 (purple) and in dashed lines, their derivatives with respect to $\mathcal{R}_0$, with $N = 100$, $\gamma = 1/3$, $S(0) = N - 1$, $I(0) = 1$, $R(0) = 0$, $M = 0.1 \cdot N$ and $\mathcal{R}_0 \in [\mathcal{R}_0{}^*, \overline{\mathcal{R}_0}]$, where $\mathcal{R}_0{}^*$ is given by Equation (11) and $\overline{\mathcal{R}_0} = 10$.

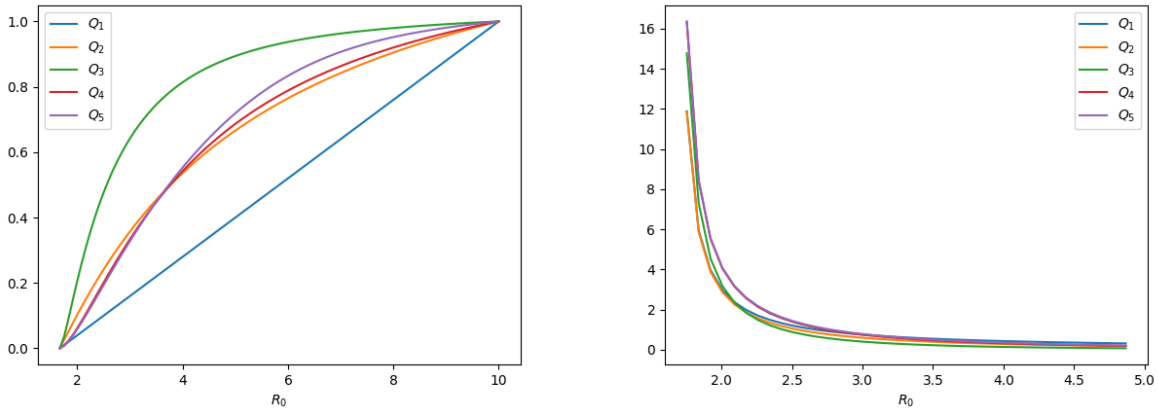

(a) Normalized Quantities

(b) Logarithmic derivatives

Figure 9: Comparison between quantities. Figure (a) shows the normalized quantities as a function of $\mathcal{R}_0$. Figure (b) shows logarithmic derivatives of the quantities, with respect to $\mathcal{R}_0$. The parameters considered were $N = 100, \gamma = 1/3, S(0) = N - 1$, $I(0) = 1, R(0) = 0, M = 0.1 \cdot N$, $\mathcal{R}_0 \in [\mathcal{R}_0^*, 10]$ in (a) and $\mathcal{R}_0 \in [\mathcal{R}_0^*, 5]$ in (b), where $\mathcal{R}_0^* \approx 1.7$ was obtained by Equation (11).

During the period under consideration, the health care capacity of Curitiba reached its maximum occupancy. To illustrate the quantification of the negative impact produced, we will use the quantity Q_4 given by Equation (16). It will be necessary to estimate the value of the health care capacity threshold.

According to the Municipal Health Department of Curitiba (SMS, 2021), the number of exclusive beds for COVID-19 in this period was around 525. In addition, 8.8 percent of the cases registered in Curitiba required hospitalization. So, we consider that $M = 525/0.088 \approx 5966$. Thus, using Equation (16), we obtain $Q_4 = 924.1690$. Figure 10(a) shows the curve of active infected individuals as a function of u (blue line), the threshold M (in red), and the quantity Q_4 for the parameters considered above.

Finally, we wanted to analyze the impact on Q_4 caused by potential reductions in $\mathcal{R}_0$ and how far the city was from *flattening* its infection curve. We considered different values of $\mathcal{R}_0$ and calculated the corresponding Q_4 values, obtaining the graph pictured in Figure 10(b). The red dot denotes the values of $\mathcal{R}_0$ and Q_4 we estimated previously for Curitiba, and the green dot corresponds to the zero impact situation obtained when $\mathcal{R}_0^* = 1.0916$ given by Equation (11). In this case, we see that to effectively flatten the curve, i.e. to achieve zero impact, a reduction of 0.1859 in the value of $\mathcal{R}_0$ would have been necessary. Note, however, that even a reduction of 0.06 in $\mathcal{R}_0$, would have flattened the curve enough to decrease the impact measured by Q_4 by approximately 80%.

5 Final Comments

Inspired by the idea of *flattening the curve* of active infected cases in an epidemic outbreak, we considered an epidemiological SIR model and a positive threshold M. We established necessary and sufficient conditions on the basic reproduction number $\mathcal{R}_0$, to ensure that the infected population does not exceed M (Proposition 2). This was achieved by using a parametric solution for the SIR model in terms of a parameter u (Equations (3)) and the properties of the Lambert W function.

We also considered the problem of quantifying the impact caused by a possible threshold exceedance, and proposed five alternatives. Quantities Q_1 (Equation (13)) and Q_2 (Equation (14)), measure the negative impact based only on considerations related to the epidemic peak. Quantities Q_3 to Q_5 quantify the global impact, by using some form of aggregation of threshold exceedances. This is done by integration with respect to the parameter t, in the case of Q_3 (Equation (15)), with respect to the parameter u, in the case of Q_4 (Equation (16)), and by a line integral over the 3-dimensional epidemic curve in the case of Q_5 (Equation (18)).

The results obtained are limited by the simplicity of the SIR epidemic model. To extend the ideas and results obtained to more complex models, some requirements would have to be satisfied. For example, to consider the SEIR model, it would be necessary to have a reparametrized solution, analogous to Equations (3) for the SIR model.

If we consider the effective reproduction number defined as $\mathcal{R}_e(t) = \mathcal{R}_0 \frac{S(t)}{N}$, some of the results can be expressed in terms

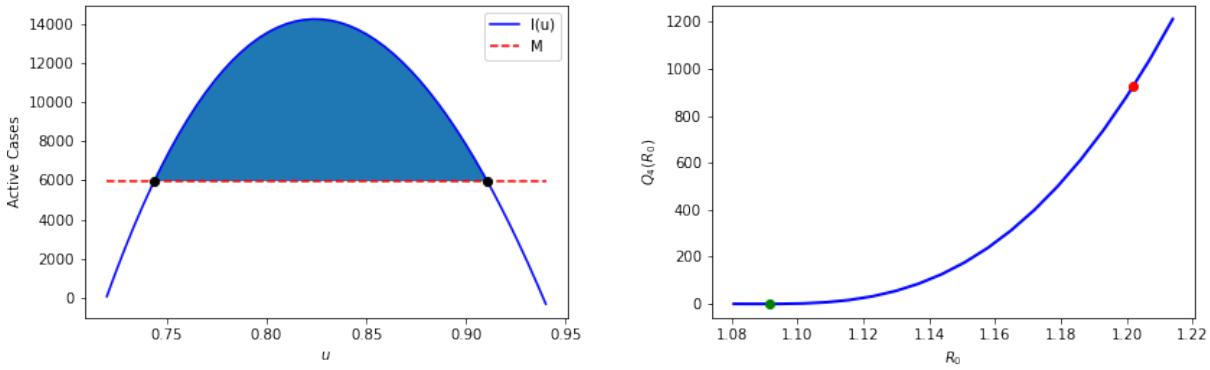

(a) Q_4 for the city of Curitiba

(b) Variation of Q_4 as a function of $\mathcal{R}_0$

Figure 10: Estimation of Q_4 for data from the city of Curitiba.

of $\mathcal{R}_\mathcal{G}(0)$ immediately. For example, Proposition (1) would become $I_{\max} \leq \frac{S}{\mathcal{R}_\mathcal{G}(0)}\left(\ln\left(\frac{1}{\mathcal{R}_\mathcal{G}(0)}\right)-1\right)-R(0)+N$ with the equality, when $\mathcal{R}_\mathcal{G}(0) \geq 1$. However, it would also be interesting to consider the effective reproductive number $\mathcal{R}_\mathcal{G}$ as an independent variable affecting the disease's dynamics. In fact, note that model (2) could be rewritten in terms of $\mathcal{R}_\mathcal{G}$. This would be a particular case of an epidemic model with variable infection rates or with infection rates depending on other variables (Greenhalgh and Das, 1995; Greenhalgh and Day, 2017; Liu and Stechlinski, 2012; Báez-Sánchez and Bobko, 2020). In this kind of situation, the curve I may not be concave or have several local optima (see Báez-Sánchez and Bobko, 2020). Hence, to obtain a result as Proposition 1, it would be necessary to consider a different approach. These issues may be considered in future studies.

A Lambert W function

The Lambert W function is a multi-valued function corresponding to the inverse relation of the function $f(x) = xe^x$. Hence, $W(x)$ gives the solutions u of the equation $ue^u = x$ i.e. $W(x)$ satisfies that

$$W(x)e^{W(x)} = x.$$

For the real case, the Lambert W function is defined only for $-\frac{1}{e} \leq x$. This and other related properties are summarized in the following lemma, given here without proof. For proof details and additional properties of the Lambert W function (see Corless et al., 1996).

Lemma 2. *For $x \in \mathbb{R}$, the Lambert W function on x is defined only for $-\frac{1}{e} \leq x$. If $-\frac{1}{e} < x < 0$, then the equation $ye^y = x$ has two solutions and, therefore, $W(x)$ has two possible values denoted by $W_{-1}(x)$ and $W_0(x)$. If $0 \leq x$, the equation has a unique solution denoted by $y = W_0(x)$. At the point $x = -\frac{1}{e}$, the equation has a unique solution $W\left(-\frac{1}{e}\right) = -1$.*

The Lambert W function can be used to solve equations involving natural logarithms as described in the following results.

Lemma 3. *Let a and b, be real numbers with $a \neq 0$. Consider the equation*

$$\ln u = au + b, \tag{21}$$

for $u > 0$. If there exist solutions, they can be expressed in terms of the Lambert W function as

$$u = \frac{W(-ae^b)}{-a}. \tag{22}$$

Equation (21) has no solutions, if $1 < ae^{b+1}$; it has two solutions, if $0 < ae^{b+1} < 1$; and it has a unique solution, if $ae^{b+1} = 1$ or $ae^b < 0$.

Proof. From Equation (21), we have that

$$\ln u = au + b \quad \Rightarrow \quad u = e^b e^{au} \quad \Rightarrow \quad -aue^{-au} = -ae^b \quad \Rightarrow \quad -au = W(-ae^b) \quad \Rightarrow \quad u = \frac{W(-ae^b)}{-a}.$$

Note that, according to Lemma 2, $W(-ae^b)$ is not defined, if $-ae^b < -\frac{1}{e}$, which is equivalent to $1 < ae^{b+1}$.This prove the first affirmation and the rest of the conditions follow in a similar way from Lemma 2. □

Lemma 4. *Let a and b, be real numbers with $b \neq 0$. Consider the equation*

$$v \ln v = av + b, \tag{23}$$

for $v > 0$. If there exist solutions, they can be expressed in terms of the Lambert W function as

$$v = \frac{b}{W(be^{-a})}. \tag{24}$$

The equation (21) has no solutions, if $be^{-a+1} < -1$; it has two solutions, if $-1 < be^{-a+1} < 0$; and it has a unique solution, if $be^{-a+1} = -1$ or $0 < be^{-a}$.

Proof. From Equation (23), we have that

$$v \ln v = av + b \quad \Rightarrow \quad -(-\ln v) = a + \frac{b}{v} \quad \Rightarrow \quad \ln\left(\frac{1}{v}\right) = -a - \frac{b}{v} \quad \Rightarrow \quad \ln u = -bu - a,$$

with $u = \frac{1}{v}$. The desired result follows from Lemma 3. □

Acknowledgments

The authors would like to thank the anonymous reviewers for their valuable comments to improve our manuscript.

References

Báez-Sánchez, A. D. and N. Bobko (2020). On equilibria stability in an epidemiological SIR model with recovery-dependent infection rate. *TEMA (São Carlos) 21*, 409 – 424. 98

Bigiani, L., S. Bigiani, and A. Bigiani (2020). How to minimize the impact of pandemic events: Lessons from the covid-19 crisis. *International Journal of Health Policy and Management 9*(11), 469–474. 85

Cooper, I., A. Mondal, and C. G. Antonopoulos (2020). A SIR model assumption for the spread of COVID-19 in different communities. *Chaos, Solitons & Fractals 139*, 110057. 85

Corless, R., G. Gonnet, D. Hare, D. Jeffrey, and D. Knuth (1996). On the Lambert W function. *Advances in Computational Mathematics 5*, 329 – 359. 86, 98

Daud, A. A. M. (2021). Comment on "poorly known aspects of flattening the curve of COVID-19". *Technological Forecasting and Social Change 167*, 120674. 85

Delamater, P. L., E. J. Street, T. F. Leslie, Y. T. Yang, and K. H. Jacobsen (2019). Complexity of the basic reproduction number (R_0). *Emerging Infectious Diseases 25*(1), 1. 87

Feng, Z., J. W. Glasser, and A. N. Hill (2020). On the benefits of flattening the curve: A perspective. *Mathematical Biosciences 326*, 108389. 85

Ferguson, N., D. Laydon, G. Nedjati Gilani, N. Imai, K. Ainslie, M. Baguelin, S. Bhatia, A. Boonyasiri, Z. Cucunuba Perez, G. Cuomo-Dannenburg, et al. (2020). Report 9: Impact of non-pharmaceutical interventions (NPIs) to reduce COVID-19 mortality and healthcare demand. *Imperial College London*. 85

Greenhalgh, D. and R. Das (1995). Modeling epidemics with variable contact rates. *Theoretical Population Biology 47*(2), 129–179. 98

Greenhalgh, S. and T. Day (2017). Time-varying and state-dependent recovery rates in epidemiological models. *Infectious Disease Modelling 2*(4), 419–430. 98

Harko, T., F. S. Lobo, and M. Mak (2014). Exact analytical solutions of the susceptible-infected-recovered (SIR) epidemic model and of the sir model with equal death and birth rates. *Applied Mathematics and Computation 236*, 184 – 194. 86, 87, 88

Heffernan, J., R. Smith, and L. Wahl (2005). Perspectives on the basic reproductive ratio. *Journal of The Royal Society Interface 2*(4), 281–293. 87

IBGE (2021). Information aggregating system of the Brazilian Institute of Geography and Statistic. https://cidades.ibge.gov.br/brasil/pr/curitiba/panorama, Last accessed on April 26, 2021. 94

Karaca-Mandic, P., S. Sen, A. Georgiou, Y. Zhu, and A. Basu (2020). Association of COVID-19-related hospital use and overall COVID-19 mortality in the USA. *Journal of general internal medicine*, 1–3. 85

Lehtonen, J. (2016). The Lambert W function in ecological and evolutionary models. *Methods in Ecology and Evolution 7*(9), 1110–1118. 86

Li, J., D. Blakeley, et al. (2011). The failure of R_0. *Computational and Mathematical Methods in Medicine 2011*. 87

Liu, X. and P. Stechlinski (2012). Infectious disease models with time-varying parameters and general nonlinear incidence rate. *Applied Mathematical Modelling 36*(5), 1974–1994. 98

Martcheva, M. (2015). *An introduction to mathematical epidemiology*, Volume 61. Springer. 87

Pakes, A. G. (2015). Lambert's W meets Kermack–McKendrick epidemics. *IMA Journal of Applied Mathematics 80*(5), 1368–1386. 86

Reluga, T. (2004). A two-phase epidemic driven by diffusion. *Journal of Theoretical Biology 229*(2), 249 – 261. 86

Rossman, H., T. Meir, J. Somer, S. Shilo, R. Gutman, A. Ben Arie, E. Segal, U. Shalit, and M. Gorfine (2021). Hospital load and increased covid-19 related mortality in Israel. *Nature Communications 12*(1). 85

SMS (2021). Municipal Health Department of Curitiba - Epidemiology Center. https://coronavirus.curitiba.pr.gov.br, Last accessed on April 26, 2021. 94, 97

Wang, A., Y. Xiao, and R. Smith (2020). Dynamics of a non-smooth epidemic model with three thresholds. *Theory in Biosciences 139*, 47–65. 86

Wang, F. (2010). Application of the Lambert W function to the SIR epidemic model. *The College Mathematics Journal 41*(2), 156–159. 86

Weiss, H. (2013). The SIR model and the foundations of public health. *Materials Matemàtics 2013*, 1887– 1907. 89

Xiao, Y., T. Zhao, and S. Tang (2013, April). Dynamics of an infectious diseases with media/psychology induced non-smooth incidence. *Mathematical Biosciences and Engineering 10*(2), 445—461. 86